Photodissociation Dynamics of Trimethylene Sulfoxide

Fei Wu, Xirong Chen, and Brad R. Weiner*

Department of Chemistry and the Chemical Physics Program, University of Puerto Rico, Box 23346 UPR Station, Rio Piedras, Puerto Rico 00931

Received: September 22, 1997; In Final Form: November 26, 1997

The photodissociation dynamics of trimethylene sulfoxide (C_3H_6SO) has been studied by monitoring the nascent SO($X\ ^3\Sigma^-$) photofragment following 193- and 248-nm irradiation by using laser-induced fluorescence spectroscopy on the $B\ ^3\Sigma^- - X\ ^3\Sigma^-$ transition. Inverted vibrational-state distributions are observed, with maxima at $v'' = 1$, for the nascent SO($X\ ^3\Sigma^-$) photoproduct for both photolysis wavelengths. Quantum yields for the production of SO($X\ ^3\Sigma^-$) are 0.34 ± 0.05 and 0.70 ± 0.14 following 193- and 248-nm photolyses of C_3H_6SO. Rotational-state distributions of the nascent SO($X\ ^3\Sigma^-$, $v'' = 1-5$) photofragment have been measured following photolysis at both wavelengths and can be characterized by Boltzmann temperatures. Energy disposal into the internal degrees of freedom of the SO($X\ ^3\Sigma^-$) photofragment is 9.9% and 11.3% of the total available energy following irradiation of the parent molecule at 193 and 248 nm, respectively. Franck−Condon and impulsive models have been used as limiting cases for the experimentally observed vibrational-state distributions and the internal energy content of the nascent SO($X\ ^3\Sigma^-$) photofragment. These models are unable to fit the experimental observations, if the other fragment is ground-state cyclopropane or propylene, but excellent agreement is obtained for the 1,3-trimethylene diradical, which is believed to be produced in the triplet state.

Introduction

Mechanisms of unimolecular reactions, both dissociation and isomerization, of small cyclic compounds have been described for many years in terms of diradical intermediates.[1] Photodissociation, defined as the electronic excitation of the parent molecule through the absorption of a photon followed by its spontaneous decay into the nascent products, has been the most widely studied of these types of reactions.[2] Measurement of the energy disposal into one of more of the nascent photofragments following photoactivation of a polyatomic molecule provides insight into the mechanistic details of the dissociation reaction.[2,3] In particular, energy-partitioning experiments have been able to provide data on transition-state structures, possible intermediates, and the nature of the interaction between the separating fragments in the exit channel. The advent of new, *direct* ultrafast pump−probe laser techniques now permits real time descriptions of these chemical reactions and has placed the diradical mechanisms under the microscope in the recent scientific literature.[4]

Internal energy distribution measurements following the photoelimination of diatoms from ring compounds, e.g. carbon monoxide from cyclic ketones, have provided a large body of mechanistic information about photochemical decarbonylations.[5] In our laboratory, we have studied the photoextrusion of sulfur monoxide from cyclic sulfoxides over the last several years.[6,7] While the cyclic sulfoxides provide an interesting analogue to the ketone photodissociations, the sulfur oxides provide a potentially richer photochemistry because of the existence of low-lying excited electronic states of SO that are energetically feasible for standard UV photolysis wavelengths.[8] Previous sulfur monoxide photoelimination studies have elucidated a variety of interesting observations, including evidence for the direct production of SO($a\ ^1\Delta$),[7] triplet ethylene,[7] and 1,4-tetramethylene diradicals.[6] We present here the results of our investigation into the photodissociation dynamics of trimethylene sulfoxide (TRSO).

The photochemistry of trimethylene sulfoxide has been studied in flash photolysis experiments by gas chromatography−mass spectrometry measurements of the stable hydrocarbon products by Dorer and Salomon.[8] For direct photolysis at 214, 229, or 254 nm, or triplet-sensitized decomposition, gaseous TRSO undergoes fragmentation to produce ethylene, propylene, and cyclopropane, with the hydrocarbon distribution depending on excitation wavelength. The hydrocarbon product distribution obtained from the photodissociation of TRSO can result from the following reactions:

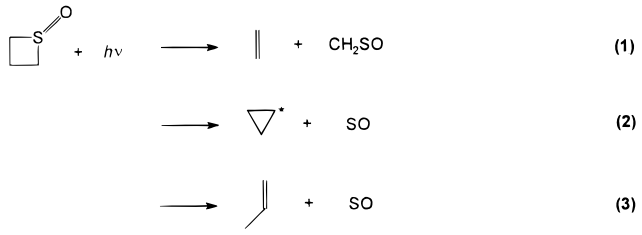

Dorer and Salomon suggested that the cyclopropane produced in reaction 2 contains sufficient vibrational energy such that it can undergo unimolecular isomerization to propylene. At higher pressures, the vibrationally excited cyclopropane can also be deactivated by energy transfer through collisions with the buffer gas. They found that the C_3H_6/C_2H_4 product ratio depended on the excitation wavelength. The lower excitation energy used in their study favored ethylene formation relative to the C_3H_6 pathway at pressures greater than 10 Torr. The authors concluded that the lifetime of the S_1 state of TRSO is sufficiently short such that photodissociation occurs more rapidly than collisional vibrational energy transfer in the pressure region below 10 Torr and proposed a mechanism based on energy

* To whom correspondence should be addressed.

S1089-5639(97)03080-6 CCC: $15.00
Published on Web 02/07/1998

partitioning, i.e., the cyclopropane versus propylene ratio as a function of bath gas collisions. Their proposed mechanism involves initial rupture of a C−S bond to produce a 1,4-trimethylene sulfinyl diradical intermediate, which subsequently fragments to yield SO(a $^1\Delta$), SO(X $^3\Sigma^-$), and the hydrocarbons. No other photochemical studies of TRSO have been reported in the literature, although the electronic structure of TRSO has been investigated both experimentally and theoretically[9,10] as a model for long-range through-bond electronic coupling in dithiaspiroalkane sulfoxides.

Scala and Colon studied the vacuum ultraviolet photochemistry of trimethylene sulfone in a flash photolysis experiment using gas chromatography to analyze the hydrocarbon products.[11] The major photolysis products at all three wavelengths are cyclopropane, propylene, and ethylene. Addition of free-radical scavengers has a marked effect upon the relative product yields, with both ethylene and propylene quenching observed following the 147-nm photolysis of TRSO in the presence of oxygen in the gas phase. The authors suggested that the primary reaction channel during the VUV photolysis of trimethylene sulfone is the elimination of SO_2 to produce a 1,3-trimethylene diradical.

Trimethylene sulfoxide is analogous to cyclobutanone. The photodissociation of trimethylene sulfoxide produces the same hydrocarbon products (ethylene, propylene, and cyclopropane) as does the photolysis of cyclobutanone.[12,13] Several studies have shown that the dissociation of cyclobutanone following excitation of the (n,π^*) transition involves two mechanistic pathways to account for the observed products.[14−16] One channel produces CO and vibrationally excited cyclopropane, while the other leads to C_2H_4 and CH_2CO. The vibrationally excited cyclopropane contains enough internal energy to isomerize to propylene, unless it is collisionally stabilized.[7] Lee and co-workers[15−17] have shown that the initial excitation into the lower vibrational levels of the S_1 manifold produces cyclobutanone, which may either fluoresce, undergo intersystem crossing to the lowest lying triplet state (T_1), or internally convert to high vibrational levels of the ground state (S_0). The primary decay channels are nonradiative since the fluorescence quantum yield is ∼0.2%. Benzene photosensitization studies have demonstrated that the T_1 state of cyclobutanone decomposes almost exclusively to cyclopropane and CO, while the ketene and ethylene products are produced from the decomposition of the singlet state of cyclobutanone.[5,9] Trentelman, et al. have studied the 193-nm photodissociation of cyclobutanone by measuring the vacuum-ultraviolet laser-induced fluorescence spectroscopy of the CO photofragment.[18] They found that the nascent rotational-state distribution of the CO($X^1\Sigma^+$) photofragment in each vibrational level ($v'' = 0-3$) can be fit well by a sum of two Boltzmann distributions with average temperatures $T_{low} = 200$ K (15%) and $T_{high} = 3000$ K (85%). These two rotational distributions were assigned to two distinct CO production pathways. The vibrational, rotational, and translational distributions of the high-temperature channel were consistent with CO and cyclopropane as the primary photoproducts. The low-temperature channel was in accord with CO produced from the unimolecular decomposition of an excited ketene intermediate. In the mechanism proposed by Trentelman et al., cyclobutanone, populated in the S_2 state by 193-nm photoactivation, undergoes internal conversion to the S_1 state, from which 57% intersystem crosses to T_1 and dissociates on the triplet surface to produce cyclopropane and a CO fragment with high rotational temperature. Another 30% of the S_1 cyclobutanone dissociates directly to produce ethylene and the first excited state of ketene, which further decomposes to yield the secondary CO fragment with a lower rotational temperature. This study clearly shows that probing the detailed internal-state distributions of the nascent CO photofragment in light of suitable physical models affords insight into the photodissociation mechanism of cyclobutanone. A detailed study of this nature has not been reported in the literature for the photodissociation dynamics of trimethylene sulfoxide.

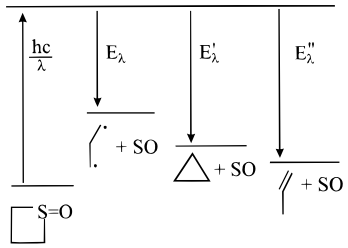

Figure 1. Schematic energy level diagram for the photolysis reactions represented by eqs 1−3.

TABLE 1: Energy Available to the Products Following Photodissociation of TRSO (Cf. Figure 1)

λ (nm)	E_λ (kcal/mol)	E_λ' (kcal/mol)	E_λ'' (kcal/mol)
193	66	119	127
248	33	86	94

Zewail and co-workers have applied femtosecond laser techniques in conjunction with mass spectrometry to study the photochemistry of cyclobutanone, cyclopentanone, and their substituted analogues.[4] They were able to observe mass signals corresponding to the 1,3- and 1,4-diradical intermediates with lifetimes on the order of 100−1500 fs. These elegant experiments clearly establish the existence of the diradicals as short-lived molecular entities.

In this work, we report our study of the UV photodissociation of trimethylene sulfoxide by probing the nascent SO(X $^3\Sigma^-$) photofragment using laser-induced fluorescence (LIF) spectroscopy on the B $^3\Sigma^-$−X $^3\Sigma^-$ transition. LIF spectroscopy of the SO(B−X) transition has been shown previously to be an excellent method for measuring ground-state sulfur monoxide internal-state distributions.[19] The experimental vibrational- and rotational-state distributions, as well as the quantum yields, of the nascent SO(X $^3\Sigma^-$) photofragment following 193- and 248-nm photolyses of TRSO are reported. There are three primary SO production channels, which are energetically allowed following 193- and 248-nm photolyses of trimethylene sulfoxide. Two of these are shown as reactions 2 and 3, and the third possibility is shown below:

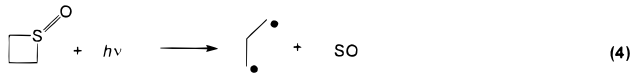

(4)

An energy level diagram for the reactions represented by eqs 2−4 is shown in Figure 1, and the energies available to be partitioned into the products at the two photolysis wavelengths are given in Table 1. The heats of formation for the species in reactions 2−4 were obtained directly from the tables when available[20] or were evaluated using thermochemical estimation methods.[21] We have modeled the vibrational-state distributions and the total energies partitioned into the internal degrees of freedom of the nascent SO photofragment following 193- and 248-nm photolyses of trimethylene sulfoxide by using a Franck−Condon/golden rule model and an impulsive model, respectively.

Experimental Section

The experimental approach has been described in detail previously and will only be outlined briefly here.[19] Trimethylene sulfoxide is stored neat in a glass trap, from which it is expanded to a partial pressure of 2−5 mTorr into a stainless steel reaction chamber. The reaction chamber is equipped with extension arms (with baffles inside to reduce scatted light) and fused SiO_2 windows. Helium buffer gas (200−300 mTorr) is flowed across the fused quartz windows to minimize the buildup of heterogeneous photolysis products. All partial and total pressures are measured at the exit of the chamber by calibrated capacitance manometers.

Trimethylene sulfoxide is photolyzed by the output of a (Lambda Physik LPX205 excimer laser, operating at either 193 nm (ArF; 6−12 mJ/cm^2) or 248 nm (KrF; 30−50 mJ/cm^2). The SO photofragments are monitored by LIF on the (B−X) transition in the 235−300-nm region of the spectrum. The probe laser light is generated by frequency doubling (β-BaB_2O_4) the fundamental (470−600 nm) of a Lambda Physik LPD3002 tunable dye laser, which is pumped by a XeCl (308-nm) Lambda Physik LPX205 excimer laser. The two laser beams, photolysis and probe, are collinearly counterpropagated along the length of the cell to maximize overlap in the center of the reaction chamber.

Fluorescence is viewed at 90° relative to the laser beam axis by a high-gain photomultiplier tube (PMT) through two long-pass filters and a band-pass filter. The output of the PMT is signal-averaged by a gated integrator and sent to a microcomputer for display, storage, and analysis. For a fixed delay time between photolysis and probe laser, the frequency-doubled output of the dye laser is scanned while collecting the total fluorescence signal to obtain a nascent LIF excitation spectrum. Data were collected at 30 Hz, with each point representing the average of 10 shots. The LIF intensity is found to be a linear function of the dye laser power, and signals taken over a large wavelength region were normalized to the dye laser power. For photolysis of trimethylene sulfoxide at either 193 or 248 nm, a linear dependence on pump laser fluence was observed, indicating that the ground-state SO is produced by a single-photon process in all cases.

Trimethylene sulfoxide was prepared by oxidation of trimethylene sulfide (Aldrich) according to the method of Kondo and Negishi.[22] The purified compound was identified by NMR analyses[23] and was subjected to three freeze−pump−thaw cycles prior to use. Sulfur dioxide and helium (Air Products, 99.9%) were used without further purification as a calibrant and a buffer gas, respectively, in the quantum yield measurements.

The vapor pressure of trimethylene sulfoxide at room temperature was measured by a calibrated capacitance manometer in a glass vacuum system. The UV absorption spectrum was measured by using a HP 8452A diode-array spectrophotometer at room temperature.

Results

Nascent SO(X $^3\Sigma^-$) photofragments are produced following both 193- and 248-nm photodissociation of trimethylene sulfoxide. A portion of a typical LIF excitation spectrum is shown in Figure 2. The assignment of the vibronic transition bands of the LIF excitation spectrum of SO(B $^3\Sigma^-$−X $^3\Sigma^-$) transition in the region of 237−300 nm was made by using the calculated bandhead positions from the spectroscopic constants in the literature.[24] The LIF excitation spectra of the SO(B $^3\Sigma^-$−X $^3\Sigma^-$) transition in the region of 237−300 nm has been used to determine the vibrational-state distributions of the nascent SO-

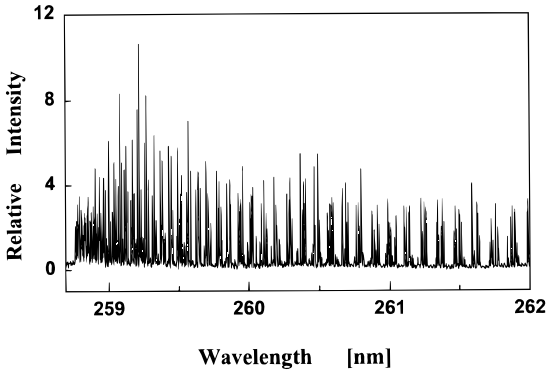

Figure 2. Rotationally resolved LIF spectrum on the SO($B^3\Sigma^-$, v'=1−$X^3\Sigma^-$, v''=3) transition following the 193-nm photolysis of trimethylene sulfoxide. P_{TRSO} = 0.005 Torr, P_{He} = 0.2 Torr, delay time = 1 μs.

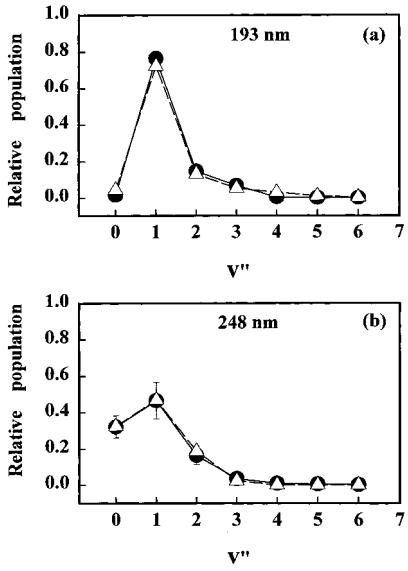

Figure 3. Experimental (●) and calculated (△) vibrational-state distributions of the nascent SO(X $^3\Sigma^-$, v'') photofragment following (a) 193-nm and (b) 248-nm photolysis of trimethylene sulfoxide.

(X $^3\Sigma^-$, v''=0−6) from the 193- and 248-nm photolyses of trimethylene sulfoxide. LIF signals, assignable to the SO (B $^3\Sigma^-$−X $^3\Sigma^-$) transition, have been recorded under collision-free conditions, where the probe delay time is less than 100 ns. The LIF spectra were measured at longer probe delay time (i.e., 1 μs) in order to avoid the interference of the emission induced by the photolysis laser. Approximately two gas kinetic collisions occur prior to detection of the SO fragment. Under these conditions, the relaxation of the nascent vibrational-state distribution of the SO(X $^3\Sigma^-$) photofragment is negligible, while the rotational-state distribution is partially relaxed.[25] The relative vibrational state populations of the SO(X $^3\Sigma^-$) photofragment in the vibrational levels v'' = 0−6 were obtained by integrating the transition bands terminating on the v' = 1 level of the B state and correcting them for the corresponding Franck−Condon factors.[26] The observed vibrational-state distributions of SO(X $^3\Sigma^-$) photofragment following 193- and 248-nm photolyses of trimethylene sulfoxide were found to be inverted with maxima at v'' = 1, as shown in Figure 3.

The rotational-state distributions of the SO(X $^3\Sigma^-$) fragment were obtained from rotationally resolved laser-induced fluorescence excitation spectra of the SO (B $^3\Sigma^-$−X $^3\Sigma^-$) transition

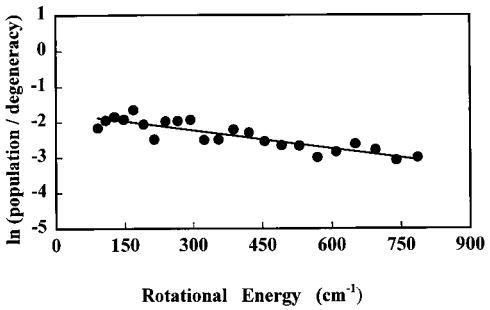

Figure 4. Boltzmann plot of the near-nascent rotational-state distribution of SO(X $^3\Sigma^-$, v''=3) resulting from the 193-nm photolysis of trimethylene sulfoxide and a linear least-squares fit to the data. The slope of the best fit line corresponds to a rotational temperature of 960 ± 170 K. The error is statistical (1σ).

TABLE 2: Rotational Temperatures of the Nascent SO(X $^3\Sigma^-$, v'') Photofragment Observed Following 193- and 248-nm Photolyses of Trimethylene Sulfoxide

	rotational temperature (K)	
vibrational level	193-nm photolysis	248-nm photolysis
1	990 ± 200	880 ± 90
2	1130 ±180	1440 ± 200
3	960 ± 170	910 ± 180
4	820 ± 150	1030 ± 180
5	800 ± 180	900 ± 160

for $v'' = 1-5$. The intensity of each assigned rovibronic transition was measured within each vibrational level and converted to the relative population by correcting for the Hönl−London factor[27] and the rotational degeneracy. We found that all the observed rotational-state distributions can be characterized by a corresponding rotational temperature. The rotational temperatures are obtained by fitting a straight line to a plot of $\ln[P(v'', N'')/(2N'' + 1)]$ vs $B_{v''}N''(N'' + 1)$, where $B_{v''}$ is the rotational constant corresponding to vibrational level v''. The Boltzmann plots for 193-nm photolysis are shown in Figure 4. The rotational temperatures of the SO photofragment are listed in Table 2.

We have also estimated the quantum yields of SO(X $^3\Sigma^-$) production at both photolysis wavelengths by comparison with the photolysis of SO_2. We have used the LIF signal of a given transition $P_{22}(13)$ of the (1, 1) band to measure the quantum yield. We recorded the LIF signal intensity originating from SO(X $^3\Sigma^-$) following the photodissociation of trimethylene sulfoxide and SO_2, respectively, under the same conditions except for the photolysis laser fluence (10 mJ/cm^2 at 193-nm photolysis and 42 mJ/cm^2 at 248 nm photolysis). The LIF intensities were averaged over 200 points and corrected to the corresponding absorption cross sections, the relative vibrational populations in the $v'' = 1$ vibrational level, and the laser fluences to yield the relative quantum yields.[19b] By comparing the relative quantum yields of SO(X $^3\Sigma^-$) from the photolysis of trimethylene sulfoxide at both 193 and 248 nm with the relative quantum yield of SO(X $^3\Sigma^-$) from the 193 nm photolysis of SO_2, we obtain the absolute quantum yields of SO(X $^3\Sigma^-$): 0.34 ± 0.05 and 0.70 ± 0.14 for 193- and 248-nm photolyses, respectively. The errors are statistical, on the basis of multiple measurements.

In previous experiments of the photodissociation of cyclic sulfoxides, direct confirmation for the production of the hydroxy radical[6] and indirect evidence for the formation of SO(a $^1\Delta$) has been found.[7] In the experiments reported here, no evidence for the production of either OH or SO(a $^1\Delta$) was observed, despite efforts made to observe these products.

TABLE 3: Best Fit Parameters Resulting from the Franck−Condon/Golden Rule Calculation of the Photodissociation of Trimethylene Sulfoxide

photolysis wavelength	193 nm	248 nm
bond length	1.501 Å	1.535 Å
bond strength	1100 cm^{-1}	1100 cm^{-1}
available energy	64 kcal/mol	33 kcal/mol

Discussion

Our experimental results indicate that trimethylene sulfoxide undergoes photoelimination of an SO(X $^3\Sigma^-$) photofragment following 193- and 248-nm irradiation. The vibrational-state distributions of the nascent SO(X $^3\Sigma^-$) photofragment following 193- and 248-nm photolyses of trimethylene sulfoxide are found to be inverted with maxima at $v'' = 1$. For a photodissociation process in which two bonds are broken, the issue of concerted versus stepwise cleavage needs to be considered. If the two bonds break in a single kinetic step, the reaction is concerted. A stepwise cleavage is defined as one which occurs in two kinetically distinct steps via an intermediate. The criteria for distinguishing between concerted and stepwise mechanisms is the lifetime of this intermediate. A lifetime equivalent to (or longer than) a single rotational period for the intermediate is the accepted criterion for labeling a photodissociation process as stepwise. The inverted vibrational-state distributions suggest that the photodissociation of trimethylene sulfoxide, at both 193 and 248 nm, proceeds via a concerted bond cleavage process in which two C−S bonds break faster than energy redistribution, i.e. less than a rotational period of the 1,4-trimethylene sulfinyl radical, to yield the SO photofragment. We cannot however conclusively rule out the possibility of a short-lived SO-containing diradical intermediate. Previous observations of inverted SO(X $^3\Sigma^-$) vibrational-state distributions following the UV photolysis of several SO containing compounds[19] have been attributed to a concerted bond cleavage mechanism.

Further insight into the photodissociation mechanisms of trimethylene sulfoxide can be obtained by comparing the experimental data in light of predictions from physical models. We have employed two approaches: (1) a Franck−Condon/golden rule model; and (2) a modified impulsive model, to simulate the total energies partitioned into the SO(X $^3\Sigma^-$) photofragment following the 193- and 248-nm photodissociation of TRSO.

The Franck−Condon/golden rule model has been used extensively to model inverted vibrational-state distributions of nascent products from elementary reactions.[19a,b,28] This model calculates the transition probability between the "dressed" diatomic oscillator, i.e. SO in the parent polyatomic molecule, and the free SO(X $^3\Sigma^-$) photofragment. If a sudden transition is assumed, the transition probability is proportional to the product of the density of the final states and the square of the corresponding Franck−Condon factor. The density of states is dependent upon the choice of available energy and, therefore, the chemical pathway. In the application of this model, we use Morse oscillator wave functions for the initial state of the "dressed" oscillator and the final state of the free SO(X $^3\Sigma^-$) photofragment. The bond length and strength of the "dressed" oscillator are treated as adjustable parameters in fitting the calculated vibrational distributions to the observed data. The best fit reveals the bond length of the "dressed" SO moiety immediately prior to fragmentation. The best fits of the calculated vibrational-state distributions to the experimental data are shown in Figure 3, and the parameters are summarized in Table 3.

TABLE 4: Comparison between Experiment and the Impulsive Model for the Energy Disposal into the Internal Degrees of Freedom of the Nascent SO(X $^3\Sigma^-$) Photofragment Following 193- and 248-nm Photolyses of Trimethylene Sulfoxide

photolysis wavelength (nm)	experimental E_v/E_{avl} (%)	E_R/E_{avl} (%)	E_{V+R}/E_{avl} (%)	impulsive model E_{V+R}/E_{avl} (%)	χ (deg)
193	6.7	3.2	9.9	10.7	34.5
248	6.4	4.9	11.3	10.7	41.6

In Table 3, the available energies correspond to eq 4 in which the SO(X $^3\Sigma^-$) photofragment is produced together with a diradical species, i.e. 1,3-trimethylene diradical. If we use available energies corresponding to the formation of the stable hydrocarbons (cyclopropane and propylene), then the Franck−Condon model cannot adequately fit the experimental data. Within the context of this model, this reveals that the SO(X $^3\Sigma^-$) photofragment is decoupled from the hydrocarbon skeleton before the stable products are formed, consistent with a concerted mechanism.

Although the SO(X $^3\Sigma^-$) photofragment is formed with a distribution of internal energies, it is useful to evaluate the average energies partitioned into the internal degrees of freedom of the SO(X $^3\Sigma^-$) photofragment for comparing with calculated energy partitioning based on a generalized impulsive model.[7] The average energy in the rotational degree of freedom can be evaluated from the rotational temperature by using $E_R = \sum c_{v''}(k_B T_{v''})/\sum c_{v''}$, where $T_{v''}$ is the rotational temperature observed in the vibrational level v'', $c_{v''}$ is the fractional population in v''. The average energy contained in the vibrational degrees of freedom can be evaluated as the sum of the energy partitioned into each vibrational level, i.e. $E_V = \sum c_{v''}(E_{v''} - E_0)/\sum c_{v''}$, where $E_{v''} = (v'' + 1/2)\omega_e + (v'' + 1/2)^2\omega_e\chi_e$ is the vibrational energy of level v'' and E_0 is the zero-point energy. The ratios of the average energies partitioned into the internal degrees of freedom of the SO fragment to the available energies are listed in Table 4.

We have used the same available energies as we used in the Franck−Condon calculation, which correspond to the reaction shown in eq 4. The observed fraction of the available energy partitioned into the internal degrees of freedom, E_{V+R}/E_{avl}, is in good agreement with the value calculated by the impulsive model as shown in Table 4. In the impulsive model calculation, the available energy is assumed to be localized on the dissociative coordinates and the bonds break rapidly so that all the available energy becomes the initial kinetic energies of the atoms on the ends of the dissociative bonds and the two photofragments decouple prior to energy redistribution between the photofragments. For a concerted dissociation, the two C−S bonds break simultaneously so that the direction of the recoil velocity of the S atom must be along the bisection of the C−S−C angle. By conservation of energy and momentum, the total energy partitioned into the internal (vibrational and rotational) degrees of freedom of the SO(X $^3\Sigma^-$) photofragment can be represented by (see Figure 5)

$$E_{V+R}(SO) = \left(1 - \frac{m_S}{m_S + m_O}\right)\frac{2m_C \cos^2\frac{\theta}{2}}{m_S + 2m_C \cos^2\frac{\theta}{2}} E_{avl} \quad (5)$$

where m_S and m_O are the masses of sulfur and oxygen atoms, respectively. θ is the C−S−C bond angle, and its experimental value[29] was used in the calculation. E_{avl} is the available energy.

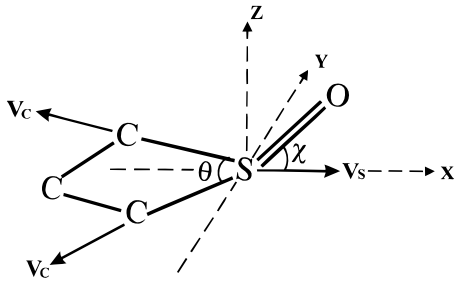

Figure 5. Geometry of trimethylene sulfoxide used in the application of the impulsive model.

If the angle between the SO bond and the C−S−C plane is χ, by analogy to the impulsive model for triatomic molecules, we have

$$E_V = E_{V+R}\cos^2\chi \quad (6)$$

$$E_R = E_{V+R}\sin^2\chi \quad (7)$$

By using eqs 6 and 7 as well as the observed values of E_V and E_R, we can evaluate the angle between the S−O bond and the C−S−C plane, χ, in the transition state of the photoactivated trimethylene sulfoxide. The results are also listed in Table 4.

The internal energy distributions of the nascent SO(X $^3\Sigma^-$) photofragment from TRSO, when taken in light of the two physical models applied here, suggest that the photodissociation of trimethylene sulfoxide following irradiation at either 193 or 248 nm proceeds via a concerted fragmentation process to produce SO(X $^3\Sigma^-$) and the 1,3-trimethylene diradical. The best fit bond lengths of the dressed SO molecule are found to be different in the 193- and 248-nm photolyses. Also the values of the angle χ in the transition state of the trimethylene sulfoxide are different in the two photolysis wavelengths. This result suggests that the dissociation of trimethylene sulfoxide may proceed on different electronic surfaces or at the different positions on the same electronic surface following 193- and 248-nm photolyses, i.e. following either internal conversion or intersystem crossing. We found that the rotational temperatures slightly increase with the increasing vibrational quantum number. The trends of the rotational temperature varying with the vibrational levels are the same for both 193- and 248-nm photolyses. It is reasonable to assume that the dissociation of the trimethylene sulfoxide occurs at different positions on the same electronic surface following 193- and 248-nm photolyses, so that the elimination of the ground-state SO at both photolysis wavelengths produces the same hydrocarbon product, i.e. the 1,3-trimethylene diradical.

By choosing the available energy in the Franck−Condon and impulsive model calculations, we have shown that the SO(X $^3\Sigma^-$) photoelimination from trimethylene sulfoxide produces the 1,3-trimethylene diradical. We cannot answer the question, based solely on these two model calculations, whether the 1,3-trimethylene diradical photofragment is produced in the singlet or triplet states. Theoretical calculations have shown that the singlet−triplet separation of the 1,3-trimethylene diradical is only about 0.8 kcal/mol.[30,31] This difference in energy is smaller than the uncertainties of these experiments and/or the physical models. The UV absorption spectrum of trimethylene sulfoxide in the gas phase shows that the absorptions at 193 and 248 nm belong to different absorption bands.[8] Absorption of a 248 nm photon promotes the trimethylene sulfoxide to the first excited singlet surface S_1, while photoexcitation at 193 nm excites the molecule to a higher singlet state.[8] If the dissociation proceeds

on the S_1 surface following 248-nm irradiation, photoelimination of the SO($X\ ^3\Sigma^-$) fragment from the trimethylene sulfoxide should produce the 1,3-trimethylene diradical in its triplet state by the conservation of spin angular momentum. To form the final hydrocarbon products, the triplet diradical must first undergo intersystem crossing (ISC) to the singlet surface.[32] Since part of the available energy is partitioned into the trimethylene diradical fragment, further fragmentation of the trimethylene diradical is also energetically allowed:

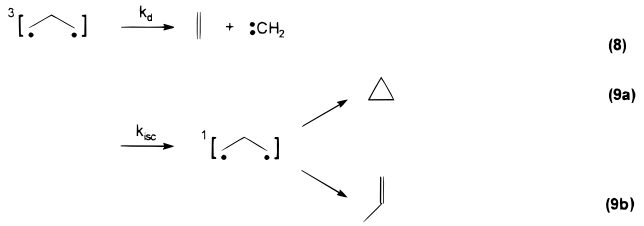

Direct observation of the 1,3-diradical by Caldwell and coworkers[33] has yielded an intersystem crossing rate of $k_{ISC} = 7 \times 10^7\ s^{-1}$. k_D can be estimated by RRK theory.[34] A typical value for the A factor for a simple fission of a C−C bond is $10^{-17}\ s^{-1}$.[21] Assuming no barrier above the endothermicity, the activation energy for reaction 8 is $E_0 = 31$ kcal/mol.[21] The maximum available energy following photolysis of TRSO at 248 nm is $E = 33$ kcal/mol. Thus, only the trimethylene diradicals produced in concert with ground vibrational state SO($X\ ^3\Sigma^-$, v''=0) have enough energy to overcome the activation barrier of reaction 8 and can undergo further fragmentation. By RRK theory, $k_d = 6.8 \times 10^9\ s^{-1}$.[33] This fragmentation rate constant is about 2 orders of magnitude larger than the reported value for k_{ISC}. This result suggests that essentially all the trimethylene diradicals produced in conjunction with the SO($X\ ^3\Sigma^-$, v''=0) fragments decompose to produce ethylene molecules and methylene diradicals (cf. eq 8). The fractional population of SO($X\ ^3\Sigma^-$) in $v'' = 0$ vibrational level indicates that 32% of the $^3C_3H_6$ diradicals can undergo further fragmentation. The remaining 68% of the triplet trimethylene diradicals, produced in conjunction with vibrationally excited SO($X\ ^3\Sigma^-$, $v'' \geq 1$), undergo intersystem crossing to the singlet state and decay rapidly to produce the C_3H_6 products, i.e. cyclopropane and propylene. Since the absolute quantum yield of trimethylene is 0.70 ± 0.14 following the 248-nm photolysis of TRSO and reaction 9 is the only pathway to produce the C_3H_6 products, the quantum yield of the C_3H_6 products should be $\Phi_{248}(C_3H_6) = 0.47 \pm 0.11$. Other reaction channels, i.e. eqs 1 and 8, produce ethylene, and their sum leads to $\Phi_{248}(C_2H_4) = 0.52 \pm 0.11$. This analysis results in a product ratio of C_3H_4/C_2H_4 produced by 248-nm photolysis of trimethylene sulfoxide of 0.88, which can be compared with previous reports. Our result agrees well with the observed product ratio of C_3H_6/C_2H_4 produced by UV photolysis of trimethylene sulfoxide at low pressure. On the basis of our quantum yield measurements of ground-state sulfur monoxide and the proposed dissociation model, the combined quantum yields of C_2H_4 and C_3H_6 following 193- and 248-nm photolysis of TRSO should not be smaller than 0.34 and 0.70, respectively. This result is different than the reported quantum yields reported by Dorer and Saloman following 253-nm photolysis.

We have studied the 193- and 248-nm photodissociation dynamics of $(CH_2)_nSO$ [where $n = 2$, 3, and 4] by monitoring the vibrational energy distributions of the nascent SO($X\ ^3\Sigma^-$) photofragment.[6,7] The nascent SO vibrational-state distributions resulting from the $n = 2$ and $n = 3$ structures are both inverted and similar. Good agreement between the experimental distributions and physical models has led us to postulate that the photoelimination of sulfur monoxide from these two compounds proceeds in a concerted manner in which the two C−S bonds break simultaneously to yield SO($X\ ^3\Sigma^-$) and unstable hydrocarbon fragments. On the other hand, the photodissociation of tetramethylene sulfoxide ($n = 5$), which yields a statistical vibrational-state distribution of SO($X\ ^3\Sigma^-$), most likely occurs via a stepwise process in which one of the C−S bonds breaks first to form a sulfinyl diradical intermediate, which subsequently dissociates to give sulfur monoxide. On the basis of these experimental results, it is clear that the ring size of the cyclic sulfoxides can affect the photodissociation mechanism. One plausible explanation may be ring strain. Thermochemical methods have shown that the ring strain for ethylene episulfoxide and trimethylene sulfoxide are ca. 83 kJ/mol, while the ring strain in the five-membered ring is only 8.5 kJ/mol.[35]

Summary and Conclusions

We have reported here the first studies of the detailed dynamics of the photodissociation of trimethylene sulfoxide. Our results and analysis are summarized as follows.

1. The nascent SO($X\ ^3\Sigma^-$) vibrational state distributions following 193 and 248 nm photolyses of C_3H_6SO show significant excitation in the diatomic photofragment (up to $v'' = 6$) and are both inverted with maxima at $v'' = 1$. The nonstatistical nature of the vibrational-state distributions of SO($X\ ^3\Sigma^-$) most likely results from the concerted cleavage of the two C−S bonds.

2. Two physical models, Franck−Condon and impulsive, have been used to model the distribution of internal energy in the SO($X\ ^3\Sigma^-$) photofragment. Both models demonstrate that a reasonable fit to the experimental data is obtained only when the other product of the photolysis is the 1,3-trimethylene diradical, and not propylene or cyclopropane.

3. Comparison of the SO($X\ ^3\Sigma^-$) quantum yields with previous hydrocarbon product distribution measurements suggests that the trimethylene diradical is initially produced in its triplet state.

4. The 248-nm photolysis promotes the trimethylene sulfoxide to its first excited singlet state S_1. Approximately 70% of the photoactivated molecules dissociate in a concerted manner on the S_1 surface to produce SO($X\ ^3\Sigma^-$) and triplet 1,3-trimethylene diradical fragments: 67.8% of the diradical $^3C_3H_6$ undergo intersystem crossing to diradical $^1C_3H_6$, leading to stable products, propylene and cyclopropane. The remaining triplet diradicals decompose to produce ethylene molecules.

Acknowledgment. The experiments performed here were done in conjunction with the Puerto Rico Laser and Spectroscopy Facility at the University of Puerto Rico, under the auspices of the NSF-EPSCoR and NIH-RCMI programs. We would like to acknowledge the generous support of this project by the Air Force Office Scientific Research through Grant F49620-93-1-0110 and by the U.S. Department of Energy (Grant No. DE-FG02-94ER75764). Partial support has also been provided by NASA through Grants NCCW-0056 and NAGW-4059.

References and Notes

(1) Dervan, P. B.; Dougherty, D. A In *Diradicals*; Borden, W. T., Ed.; Wiley: NewYork, 1982; pp 107−149.

(2) See for example: *Molecular Photodissociation Dynamics*; Ashfold, M. N. R., Baggott, J. E.; Eds.; Royal Society of Chemistry: London, 1987. Schinke, R. *Photodissociation Dynamics*; Cambridge University Press: Cambridge, 1993.

(3) Butler, L. J.; Neumark, D. M. *J. Phys. Chem*. **1996**, *100*, 12801.
(4) Pedersen, S.; Herek, J. L.; Zewail, A. H. *Science* **1994**, *266*, 1359.
(5) (a) Jimenez, R.; Kable, H. S.; Loison, J.-C.; Simpson, C. J. S. M.; Adam, W.; and Houston, P. L. *J. Phys. Chem*. **1992**, *96*, 4188. (b) Trentelman, K. A.; Moss, D. B.; Kable, S. H.; Houston, P. L. *J. Phys. Chem.* **1990**, *94*, 3031. (c) Sonobe, B. I.; Fletcher, T. R.; Rosenfeld, R. N. *J. Am. Chem. Soc.* **1984**, *106*, 4352−4356, 5800−5805. (d) Sonobe, B. I.; Fletcher, T. R.; Rosenfeld, R. N. *Chem. Phys. Lett.* **1984**, *105*, 322, (e) Prather, R. A.; Rosenfeld, R. N. *J. Phys. Chem.* **1991**, *95*, 6544.
(6) Wu, F.; Chen, X.; Weiner, B. R. *J. Phys. Chem*. **1995**, *99*, 17380.
(7) Wu, F.; Chen, X.; Weiner, B. R. *J. Am. Chem. Soc*. **1996**, *118*, 8417.
(8) Dorer, F. H.; Salomon, K. E. *J. Phys. Chem*. **1980**, *84*, 3024.
(9) Baker, A. D.; Scharfman, R.; Srein, C. A. *Tetrahedron Lett*. **1983**, *24*, 2957.
(10) Rendell, A. P.; Basckay, G. B.; Hush, N. S. *J. Am. Chem. Soc*. **1988**, *110*, 8343.
(11) Scala, A. A.; Colon, I. *J. Phys. Chem*. **1979**, *83*, 2025.
(12) Lee, N. E.; Lee, E. K. C. *J. Phys. Chem*. **1969**, *50*, 2094.
(13) (a) Denschlag, H. O.; Lee, E. K. C. *J. Am. Chem. Soc*. **1968**, *90*, 3628. (b) Carless, H. A. J.; Metcalf, J.; Lee, E. K. C. *J. Am. Chem. Soc*. **1972**, *94*, 7221. (c) Tang, K. Y.; Lee, Y. P.; Schaefer, H. F. *J. Chem. Phys*. **1979**, *71*, 3761.
(14) (a) Campbell, R. J.; Schlag, E. W.; Ristow, B. W. *J. Am. Chem. Soc*. **1967**, *89*, 5098. (b) Campbell, R. J.; Schlag, E. W. *J. Am. Chem. Soc*. **1967**, *89*, 5203.
(15) (a) Klemm, R. F.; Morrison, D. N.; Gilderson, P.; Blades, A. T. *Can. J. Chem*. **1965**, *43*, 1934. (b) Hemminger, J. C.; Lee, E. K. C. *J. Chem. Phys.* **1972**, *56*, 5284. (c) Tang, K. Y.; Lee, E. K. C. *J. Phys. Chem*. **1976**, *80*, 1833.
(16) Hemminger, J. C.; Rusbult, C. F.; Lee, E. K. C. *J. Am. Chem. Soc*. **1971**, *93*, 1867.
(17) Shortridge, R. G.; Yang, W.; Lee, E. K. C. *Mol. Photochem*. **1969**, *1*, 325.
(18) Trentelman, K. A.; Moss, D. B.; Kable, S. H.; Houston, P. L. *J. Phys. Chem*. **1990**, *94*, 3031.
(19) (a) Wang, H.; Chen, X.; Weiner, B. R. *Chem. Phys. Lett.* **1993**, *216*, 537. (b) Wang, H.; Chen, X.; Weiner, B. R. *J. Phys. Chem.* **1993**, *97*, 12260. (c) Chen, X.; Wang, H.; Weiner, B. R.; Hawley, M.; Nelson, H. H. *J. Phys. Chem.* **1993**, *97*, 12269. (d) Barnhard, K. I.; Santiago, A.; He, M.; Asmar F.; Weiner, B. R. *Chem. Phys. Lett.* **1991**, *178*, 150.
(20) Lide, D. R., Kehiaian, H. V., Eds. *CRC Handbook of Thermophysical and Thermochemical Data*; CRC: Boca Raton, FL, 1994; pp 125−169.
(21) Benson, S. W. *Thermochemical Kinetics, Methods for the Estimation of Thermochemical Data and Rate Parameters*, 2nd ed.; Wiley-Interscience: New York, 1976.
(22) Kondo, K.; Negishi, A. *Tetrahedron* **1971**, *27*, 4831.
(23) Rasheed, K.; Warkentin, J. D. *J. Org. Chem.* **1980**, *45*, 4807.
(24) Colin, R. *J. Chem. Soc., Faraday Trans. 2* **1982**, *78*, 1139.
(25) Chen, X.; Wu, F.; Weiner, B. R. *Chem. Phys. Lett.* **1995**, *247*, 313.
(26) Smith, W. H.; Liszt, H. S. *J. Quant. Spectrosc. Radiat. Trans.* **1975**, *11*, 45.
(27) Tatum, J. B. *Can. J. Phys.* **1966**. *44*, 2944.
(28) (a) Berry, M. J. *Chem. Phys. Lett.* **1974**, *29*, 323, 329. (b) Chen, X.; Asmar, F.; Wang, H.; Weiner, B. R. *J. Phys. Chem.* **1991**, *95*, 756. (c) Berry, M. J.; *J. Chem. Phys.* **1974**, *39*, 3114. (d) Schatz, G. C.; Ross, J. *J. Chem. Phys.* **1977**, *66*, 1037. (e) Mukamel, S.; Jortner, J. *J. Chem. Phys.* **1974**, *60*, 4760.
(29) Bevan, J. W.; Legon, A. C.; Millen, D. *J. Proc. R. Soc. (London)* **1977**, *A354*, 491.
(30) Yamaguchi, Y.; Schaefer, H. F. *J. Am. Chem. Soc*. **1984**, *106*, 5115.
(31) Yamaguchi, Y.; Osamura, Y.; Schaefer, H. F. *J. Am. Chem. Soc*. **1983**, *105*, 7506.
(32) Carlacci, L.; Doubleday, C.; Furlani, T. R.; King, H. F.; McIver, J. W. *J. Am. Chem. Soc.* **1987**, *109*, 5323.
(33) Mizuno, K.; Ichinose, N.; Otsuji, Y.; Caldwell, R. A. *J. Am. Chem. Soc*. **1985**, *107*, 5797.
(34) Robinson, P. J.; Holbrook, K. A. *Unimolecular Reactions*; Wiley-Interscience: New York, 1971.
(35) Herron, J. T. in *The Chemistry of Sulphones and Sulphoxides*; Patai, S., Rappoport, Z., Stirling, C., Eds.; John Wiley and Sons: New York, 1988; pp 95−106.